18TH WORLD CONFERENCE ON EARTHQUAKE ENGINEERING
WCEE2024
MILAN

MILAN, ITALY
30TH JUNE - 5TH JULY 2024
www.wcee2024.it

SURROGATE MODEL FOR FRAGILITY ASSESSMENT OF RETROFITTED UNREINFORCED MASONRY BUILDINGS

A. FathiAzar[1], S. Alfano[1] & S. Cattari[1]

[1] University of Genoa - Department of Civil, Chemical and Environmental Engineering, Genova, Italy, abbas.fathiazarkalkhoran@edu.unige.it

Abstract: *This work presents an efficient computational framework that relies on surrogate modeling and machine learning methods to estimate seismic fragility parameters for different typologies of Unreinforced Masonry buildings (URM) subjected to different retrofitting scenarios. The presented model is part of a decision support tool that aims to assist various stakeholders in assessing different intervention scenarios for a city-wide building portfolio. The model utilizes a Gaussian Process (GP) that is trained to map the URM capacity curves in their as-built and retrofitted states with parameters of fragility functions (median and standard deviation). Three hundred ninety capacity curves for different URM typologies (Un-retrofitted and retrofitted) are generated using the DBV-Masonry model, which was developed at the University of Genoa. The model belongs to the analytical-mechanical approach and, within the context of the MARS (MAps of Seismic Risk) ReLUIS project, has been extensively used in large-scale risk studies and validated against observed data from Italian seismic events. These capacity curves are then utilized to produce equivalent single-degree-of-freedom models to represent the structural behavior. Fragility curves are then developed using nonlinear time history analysis and a modified cloud-based approach and used to train the GP model. Overall, deploying the proposed model can significantly improve the decision-making process for building portfolio management in seismic-prone regions by providing a fast and efficient way of evaluating retrofit strategies.*

1 Introduction

In the past few years, there has been a shift in scholarly attention transitioning from just developing fragility curves for existing buildings to the assessment of interventions' influence on the enhanced performance of buildings and the consequent alterations in fragility curves. These studies are typically conducted at three different scales: the element level (Sistani Nezhad, Kabir and Banazadeh, 2022; Jafari and Mahini, 2023; Yurdakul *et al.*, 2023), individual building/asset scale (Padgett and DesRoches, 2008; DA PORTO *et al.*, 2022; Blasi, Perrone and Aiello, 2023) and the portfolio level (Ferreira, Maio and Vicente, 2017; Cattari *et al.*, 2022; Hoyos and Silva, 2022; Kalakonas and Silva, 2022; Pietro, Veronica and Marco, 2023). This shift also manifested itself in practical projects; for example, the assessment of the potential reduction in risk through retrofit interventions has been addressed in the ReLUIS[1] project called MARS (**S**eismic **R**isk **Ma**ps), carried out between 2019 and 2021. This investigation is currently ongoing through the MARS2 project, which extends from 2022 to 2024 (Follador *et al.*, 2023).

[1] Consortium of the Network of University Laboratories of Earthquake and Structural Engineering (https://www.reluis.it/en/)

Similar to the derivation of fragility curves, these studies can be conducted either through observations made after the earthquake event and evaluation of the performance of retrofitted buildings (Saretta, Sbrogio and Valluzzi, 2021) or using analytical methods. The former approach offers an improved understanding of the performance, potential advantages, and limitations of intervention measures, but the lack of available data limits its applicability to all building typologies and different earthquake intensities. Hence, there are some added values in using analytical approaches. Nevertheless, these methods also have some drawbacks. For example, they lack the characteristics necessary for seamless integration into a Multi-Hazard Decision Support Tool (DST) that requires fast assessment of various interacting hazard scenarios combined with dynamic vulnerabilities.

The authors are currently developing a DST that aims to conduct comparative city-wide Multi-Hazard Risk Analyses by assessing the effectiveness of different retrofit strategies and their Synergies and A-synergies in a multi-hazard landscape. This paper elaborates on the masonry part of DST's Seismic Risk module that facilitates the portfolio scale risk assessment through Machine Learning (ML) based surrogate models. The purpose of the model is to substitute complex and time-consuming numerical Nonlinear Time History Analysis (NLTH) with a simple ML-based model. This substitution aims to reduce the computational load involved in city-wide risk assessment studies with different scenarios of structural interventions in which utilizing NLTH for all structures is impractical and where an approximate but dependable representation of the NLTH is satisfactory. We begin by providing a broad introduction to our metamodel, which consists of various subordinate models. Subsequently, we provide an in-depth explanation for each of these individual models.

2 Development of metamodel

As a general definition, a metamodel is a model comprising other models that are related to each other. In other words, a metamodel is itself a model, but it pertains specifically to a set of models deemed significant for the final goal. Within the context of this paper, the metamodel, as depicted in Figure 1, aims to predict the fragility function parameters of the retrofitted buildings using their enhanced capacity curves. The changes in the capacity curve will be identified by an Analytical-Mechanical Procedure named DVB-Masonry (elaborated in sec 2.1) and then fed into a Gaussian Process Regression module, which will predict the fragility parameters.

Several models have been documented in the literature that can predict fragility curves for masonry buildings in their as-built and retrofitted condition. For instance *DVB-Masonry* (Cattari et al., 2021), *Vulnus* (Bernardini, Gori and Modena, 1990; Valluzzi, Follador and Sbrogiò, 2023), and the macroseismic-heuristic procedure (Lagomarsino and Giovinazzi, 2006), among others. However, when compared with other simplified methods, this surrogation model has some advantages. For example, due to its flexibility to be trained using different input parameters, it can be formulated to consider different Intensity measures (IMs) or Engineering Demand Parameters (EDPs). Furthermore, since it is trained using the results of Nonlinear Time History Analysis (NLTHA), it inherits the advantages that come with such analysis.

The metamodel (Figure 1) encompasses three main models:

1. An enhanced *DBV-Masonry* model, which is formulated using an analytical-mechanical approach. In this study, the DVB-Masonry model is chosen because (i) in addition to fragility curves, it provides capacity curves of the masonry buildings (which we have used in this study), and (ii) it considers the Out-of-Plane (OoP) mechanisms in defining the capacity curves and damage state limits, distinguishing it from other approaches.
2. An Openseespy (Zhu, McKenna and Scott, 2018) subroutine to perform cloud (and Cloud to IDA) analysis (Jalayer, De Risi and Manfredi, 2015) on a series of equivalent Single Degree of Freedom oscillators (SDoF).
3. Gaussian Process Regression models (Rasmussen and Williams, 2006) that are trained to map the capacity curve parameters to the fragility parameters.

The components of the model are elaborated in the following subsections.

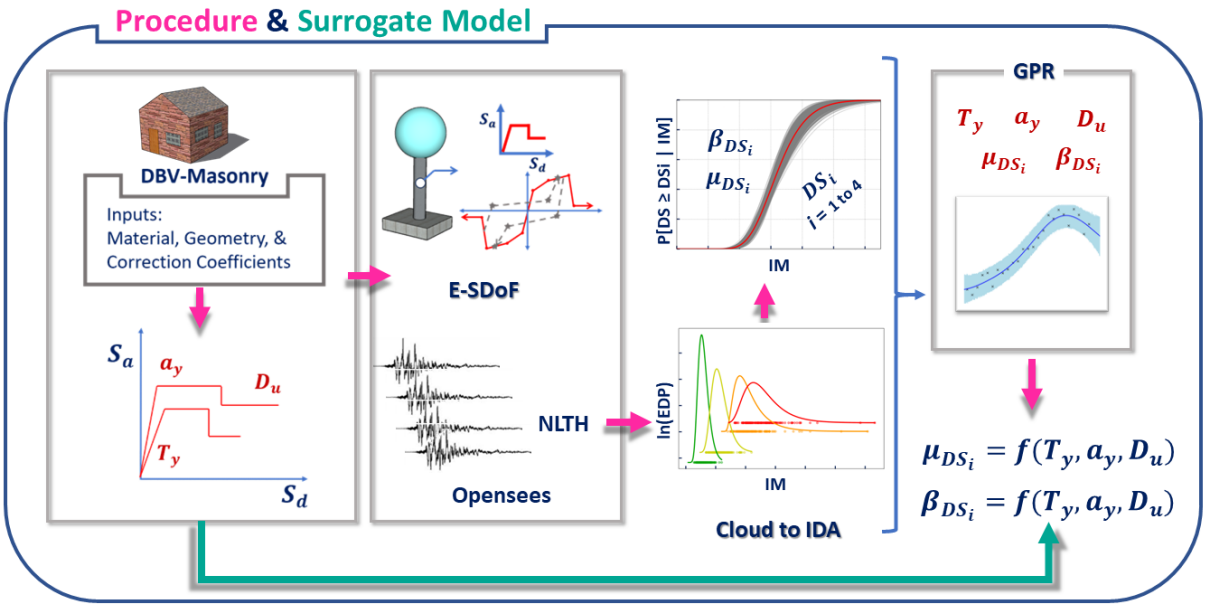

Figure 1. The procedure for training the GP model (red) and the final Surrogate mode (green)

2.1 Analytical-Mechanical Procedure (DBV-Masonry)

Model description

This model, which is also implemented within the MARS project (Cattari et al., 2021), is an improved version of the original DBV-Masonry model (Lagomarsino and Cattari, 2014). The original model aimed to establish fragility functions assuming a box-type behavior of URM buildings concerning just the in-plane response of the walls. However, the enhanced DBV-Masonry model can also consider the activation of OoP mechanisms (DA PORTO et al., 2022). This is achieved by incorporating corrective coefficients that limit the displacement capacities corresponding to DL3 and DL4. These coefficients are a function of masonry and diaphragm types (Cattari *et al.*, 2021). The model first establishes the capacity curve, which represents the structural seismic response and is defined using three variables:

- The pseudo-elastic period of the structure, T_y.
- The spectral acceleration at yielding, a_y, which is assumed to be constant up to spectral displacement associated with Damage state 3 (no hardening is considered).
- The ultimate displacement capacity, D_u, which indicates the maximum displacement that the structure can withstand.

In order to calculate these variables, in addition to assuming a fundamental mode shape, only a small number of mechanical and geometrical parameters need to be specified. However, the model employs over ten corrective factors (K_i) to account for various constructive and morphological characteristics specific to different building types within a portfolio and different damage mechanisms. The original damage mechanism used to formulate the model (without corrective factors) is the Strong-Spandrels Weak-Piers (SSWP) mechanism. However, the model can consider other mechanisms, such as WSSP (Weak-Spandrels Strong-Piers) or any arbitrary intermediate behavior.

Next, the model employs the concept of over-damped spectra to calculate the value of the Intensity Measures (IMs) that correspond to achieving various damage levels. This process also involves considering different types of uncertainties.

Changes in capacity curves due to intervention

In the DBV-Masonry, the effects of retrofit implementation are evaluated in two ways:

- Enhancing the mechanical properties of masonry through corrective coefficients, which are derived from Table C8.5.II of the Italian Circular 2019/01/21 (Italian Ministry of Infrastructures and Transports, 2019).

- Increasing the overall ductility of the capacity curve for DL3 and DL4. This increase can be attributed to the positive impact these interventions have on OoP mechanisms in the case of irregular masonry or the expected improvement in drift thresholds for solid brick masonry.

It should be emphasized that when multiple interventions are implemented, the coefficients are modified to consider the potential reduction in effectiveness that may arise from combining interventions. Additionally, since some of these interventions involve the incorporation of materials, it was estimated that there would be an average increase in the specific weight of masonry. In the case of stone masonry, the estimated increase is approximately 5%, while for solid and hollow brick masonry, it is around 4%. Figure 2 presents a schematic of intervention measures that were used in this study: (i) An intervention focused on improving connections (HQD-TR or HQD-RC); (iii) An intervention aimed at stiffening the floors (FLR).

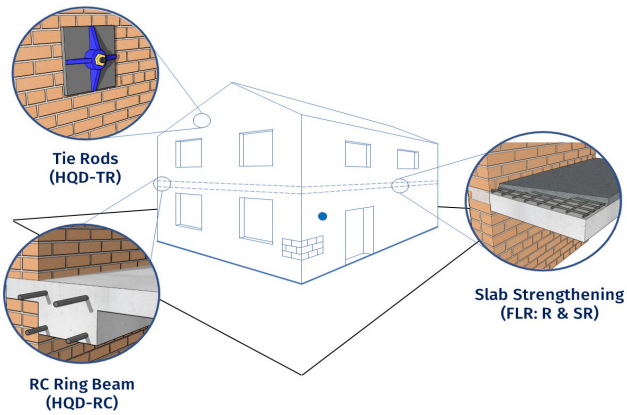

Figure 2. Schematic presentation of intervention methods considered in this study

DBV Taxonomy

As presented in Table 1, DBV considers a relatively detailed taxonomy with four groups of attributes (pertaining to as-built and retrofitted buildings). These typologies can later be aggregated to generate other taxonomies with smaller attributes.

Table 1. Attributes of DBV Taxonomy

Attribute	Possible values	Abbreviation
Number of floors	1-4	-
Construction details	Low-Quality Details	LQD
	High-Quality Details with Tie Rods	HQD_TR
	High-Quality Details with R.C. Ring Beams	HQD_RB
Masonry types	**Regular**	
	Stone ashlar	HSRC
	Soft Stone	SS
	Block masonry	HS
	Solid bricks	FB
	Hollow blocks	HC(L%)
	Modern masonry	CMU or AAC
	Fragile hollow blocks	HC(H%)
	Irregular	
	Rubble stone	HSRU
	Stone ashlar	HSUC
	Soft stone	SSUC
Slab type	Vaults	V
	Flexible	F
	Semi-rigid	SR
	Rigid	R

2.2 The SDoF models

In this study, 390 SDoF systems were defined (presenting both un-retrofitted and retrofitted buildings). The capacity curve for each building is used to define the backbone curve of the SDoF. The hysteretic behaviour of the SDoF is characterized by pinching4 material model in openseespy (Zhu, McKenna and Scott, 2018). To calibrate the model parameters, the results of cyclic pushover of a URM building that has been modeled in TREMURI software (Lagomarsino *et al.*, 2013) were used. Although the cyclic push results didn't demonstrate a severe pinching behavior, we used pinching4 for its ability to model strength and stiffness reduction abilities, its flexibility, and then adjust the pinching behavior according to the cyclic pushover results. The modifications of material properties, as well as analysis procedure and fragility derivations (section 2.4), are implemented in the freely available Vulnerability Modellers ToolKit (VMTK) (Martins *et al.*, 2021) source code.

2.3 Analysis method and derivation of fragility functions

Fragility Derivation

We started our investigation using original cloud method (Jalayer *et al.*, 2017) which consists of (i) performing a large number of nonlinear dynamic time–history analyses and extracting Engineering Demand Parameters (EDPs) corresponding to the Intensity Measure (IM) of each record, (ii) constructing a probabilistic seismic demand model (PSDM) (Cornell *et al.*, 2002) that expresses the relation between IM-EDP and follows a double-logarithmic linear distribution as expressed in Equation (1) that can be used to extract the median of fragility curve for different damage states; (iii) and finally the dispersion which is assumed as constant for all damage states is driven using the Equation (2). Since we were dealing with a SDoF system, maximum displacement was selected as EDP, and since we wanted our results to be applicable to a portfolio of buildings, Peak Ground Acceleration (PGA) was selected as IM.

$$E[\ln D_{max}|\mathrm{PGA}] = \ln a + b\ln \mathrm{PGA} \tag{1}$$

Where $E[\ln D_{max}|\mathrm{PGA}]$ is the expected value for the logarithm of maximum displacement (D_{max}) given PGA; $\ln a$ and b are parameters of linear regression;

$$\beta_d = \sqrt{\sum_{i=1}^{N}(\ln \mathrm{D}_{max_i} - \ln \mu_d)^2 \,/\, \sum_{i=1}^{N}(\ln \mathrm{D}_{max_i} - \ln \mu_d)^2 (N-2)(N-2)} \tag{2}$$

β_d is the logarithmic standard deviation of D_{max} given the IM=PGA; μ_d is $E[\ln D_{max}|\mathrm{PGA}]$; D_{max_i} is the D_{max} obtained from the *i* th record, and N is the number of records.

This procedure, however, had some problems when analyzing very stiff and high-strength typologies. The cloud points demonstrated a bi-linear trend in log-log space, and fitting a linear relation (Equation (1)) to the cloud data resulted in unrealistic medians for higher damage states. Hence, we moved to a modified cloud method (Cloud to IDA procedure) (Miano *et al.*, 2018). This method is a combination of Incremental Dynamic Analysis (IDA) and cloud analysis. Similar to IDA, the method drives the fragility curves using the PGA values corresponding to the displacement levels where the displacement is equal to the damage state threshold ($DCR_{DSi} = 1$). For demonstration purpose the data points for different damage states pertaining a 3 story building is shown in Figure 3.

In this method, unlike IDA, the starting point of analysis for each TH is the unscaled condition of that TH, and the algorithm is allowed to scale these THs with a limited scaling factor (in this study, we used 2.5). This procedure allows obtaining the IDA curves with very few analyses and, at the same time, doesn't have the problems of the original IDA method, which were caused by excessive scaling. For a given set of THs, there is always a trade-off between the maximum scaling factor and the number of THs that can cause the demand equal to the damage state threshold. The number of such THs will be even smaller for the highest damage states and stiff structures, which necessitate a relaxed scaling factor for such scenarios.

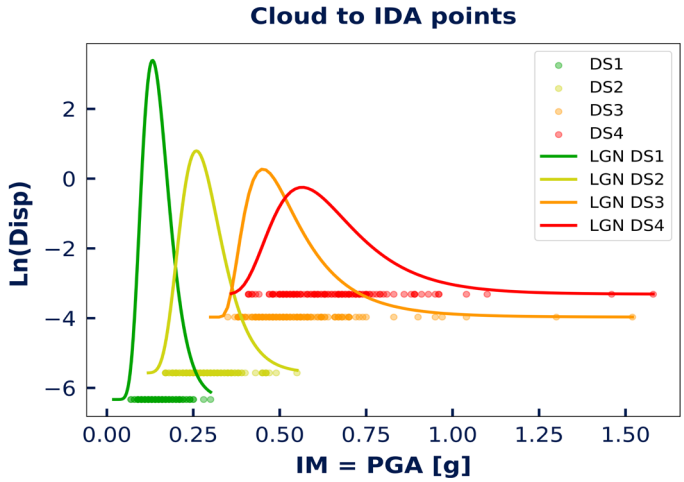

Figure 3. An example of final Cloud-to-ID points with a maximum scaling factor of 2.5

Figure 4 presents a set of fragility curves that have been driven for one of the mentioned buildings using the bootstrapping method (Baraschino, Baltzopoulos and Iervolino, 2020).

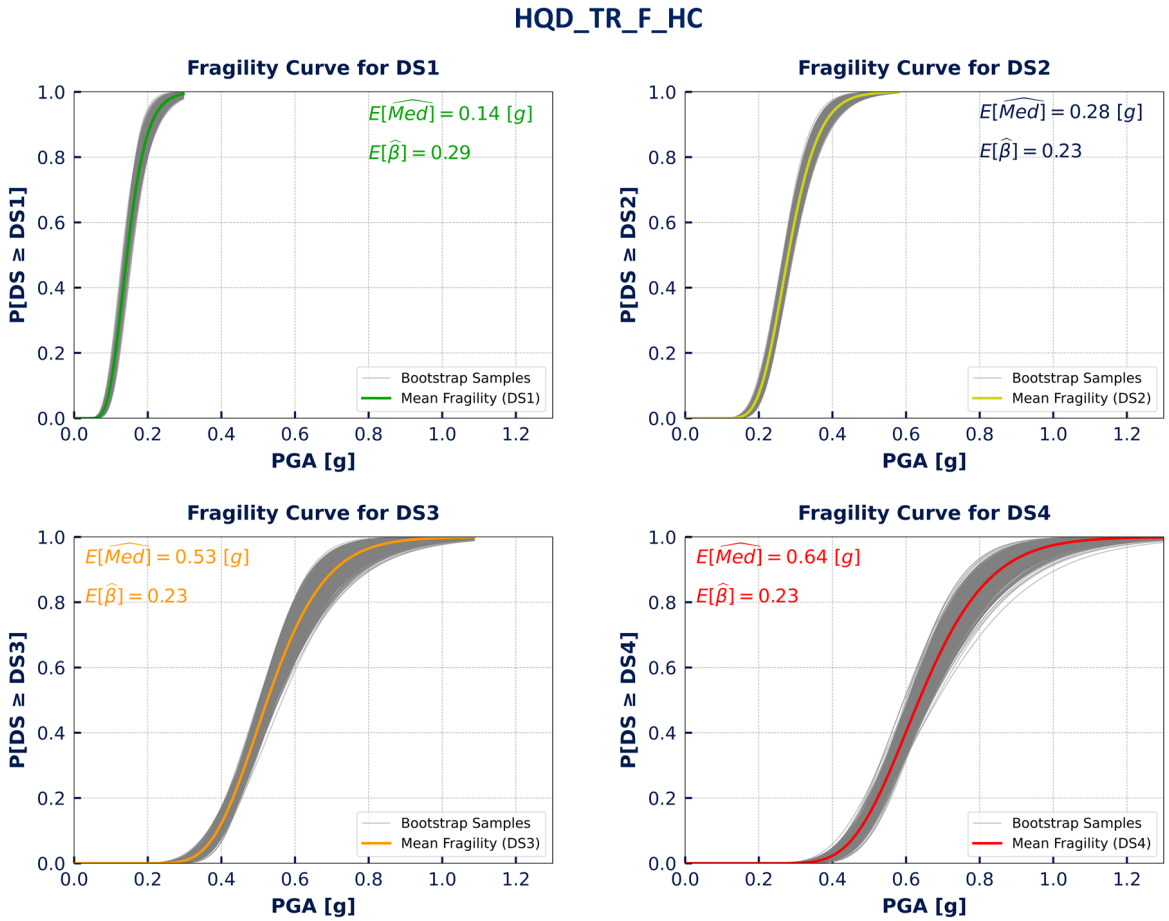

Figure 4. An example of a set of fragility curves and bootstrap realizations (in gray)

These fragility curves are checked with the ones that have been used in seismic risk assessment of Italy (da Porto *et al.*, 2021) and have acceptable agreement. It is worth mentioning that the standard deviation that results from this procedure is related to Record-to-Record variability (β_{R2R}) and it should be combined with other uncertainties (as required) to be applicable in the risk assessment procedure. This combined standard deviation (β_{ToT}) usually can be calculated using Equation (3).

$$\beta_{ToT} = \sqrt{\sum \beta_i^2} \tag{3}$$

Where β_is are different uncertainties (for example, inter-building and intra-building uncertainties).

Unscaled TH set

In this study, time histories (THs) selected by (Manfredi *et al.*, 2022) for stiff soil are utilized, which facilitates the derivation of site-independent fragility curves through a cloud-based methodology. The magnitude-distance characteristics of the 125 earthquake events (AB set), along with their Acceleration Displacement Response Spectrum (ADSR) are depicted in Figure 5. The capacity curve of one building in pre- and post-intervention scenarios are also depicted in the figure for demonstration purpose.

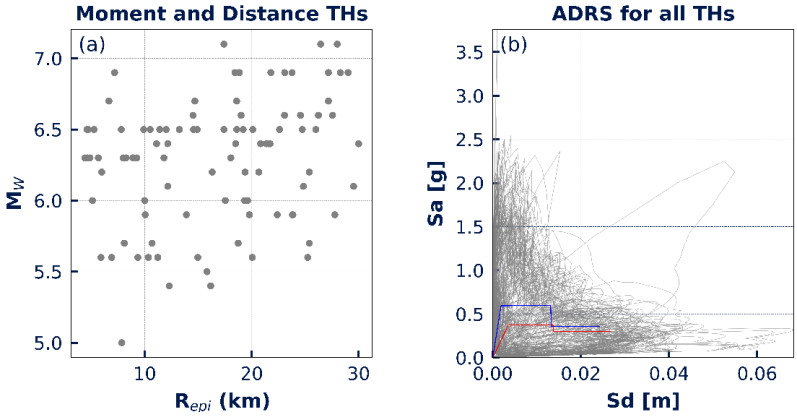

Figure 5. Characteristics of selected THs (a) M-R distribution, (b) ADRS of all THs

2.4 Gaussian process

Gaussian process (GP) is a data-driven method that offers the ability to model intricate physical systems with exceptional flexibility, all while bypassing the need to assume a specific functional form. This model allows for the assessment of expected values and their corresponding uncertainties, which are dependent on input variables and exhibit heteroscedasticity. (Rasmussen and Williams, 2006; Zhong *et al.*, 2020; Delaviz and Yaghmaei-Sabegh, 2023). GP has been used for different purposes in earthquake engineering, for example, for predicting Ground-Motion Time Series (Tamhidi *et al.*, 2022), spatial correlation of ground motion IMs (Kuehn and Abrahamson, 2020), or development of non-ergodic earthquake ground-motion models (Lavrentiadis *et al.*, 2022). There are also some studies that have used this method to assess seismic risk or specifically to drive fragility parameters from structural parameters related to RC buildings (Minas, Chandler and Rossetto, 2018; Gentile and Galasso, 2020; Sarli *et al.*, 2022), steel buildings (Fayaz *et al.*, 2023), base-isolated buildings (Zhong *et al.*, 2020; Delaviz and Yaghmaei-Sabegh, 2023; Suarez *et al.*, 2023) or for bridges (Zhong *et al.*, 2020; Pang *et al.*, 2021).

With reference to Equation (4), a Gaussian process is a probability distribution $P(f)$ over continuous functions $f(\boldsymbol{x})$, where any subset of function values $f(\boldsymbol{x})$ follows a joint multivariate Gaussian distribution with a mean function $m(\boldsymbol{x})$ and covariance matrix $k_{xx'} = k(\boldsymbol{x}, \boldsymbol{x}')$(Rasmussen and Williams, 2006; Schulz, Speekenbrink and Krause, 2018).

$$f(\boldsymbol{x}) \sim \mathcal{GP}(m(\boldsymbol{x}), k(\boldsymbol{x}, \boldsymbol{x}')) \tag{4}$$

The covariance function $k(\boldsymbol{x}, \boldsymbol{x}')$ encodes the properties of the function, such as smoothness, and can vary based on the chosen kernel and its parameters or hyperparameters (denoted as θ). In order to explicitly indicate the reliance on $k(\boldsymbol{x}, \boldsymbol{x}')$ on these (hyper)parameters (θ), the covariance function is commonly expressed as $k(\boldsymbol{x}, \boldsymbol{x}'|\theta)$ (MathWorks, 2023).

As explained previously, GP is a prior distribution over possible functions. In the context of this paper, it is assumed that the median and standard deviation of fragility functions are functions of the capacity curve parameters. Due to the unknown and complicated functional forms, they are replaced with a set of GPs. To estimate the fragility parameters, the GPR is trained using the observed values, f, which represent the median

and standard deviation of fragility functions for different damage states as a function of capacity curve parameters X. Then, the prediction of fragility parameters (f_{new}) based on a new capacity curve data x_{new}, can be made using the Equation (5):

$$f_{new}|f, X, x_{new} \sim \mathcal{N}\ (m_{new}, \Sigma_{**}) \tag{5a}$$

$$m_{new} = m + k_{Xx_{new}}\ k_{XX}^{-1}\ (f - m) \tag{5b}$$

$$\Sigma_{**} = \ k_{x_{new}x_{new}} - \ k_{x_{new}X}\ k_{XX}^{-1}\ k_{Xx_{new}} \tag{5c}$$

In which:

The X is the capacity curve parameters used for training, x_{new} is the input parameters of new capacity curve parameters for which fragility curve parameters are going to be calculated; $k_{Xx_{new}}$ describes the covariance between the input capacity curve parameters and the new ones, $k_{x_{new}x_{new}}$ is the covariances of the new capacity curve parameters m and m_{new} are the prior mean vectors for the training and new capacity curve parameters, respectively.

3 Model training and performance

Training

To train the model, a tenfold cross-validation approach is utilized, where the data is divided into ten mutually exclusive subsets through stratified sampling. This process ensures that each subset is used as a test set once, while the remaining nine subsets are used for training and reduce the probability of overfitting. The parameters are estimated on 90% of the data during each training phase. The results from the ten iterations are then averaged. In addition to the k-fold approach, the capacity curve data of 10 buildings with different characteristics were separated and used as test data after the training procedure.

Covariance functional

The output function of a Gaussian process exhibits smoothness, meaning that a slight change in the input will lead to a correspondingly small perturbation in the output. To ensure the smoothness of a Gaussian process, it is essential to define an appropriate covariance functional form that governs the relationship between process values at different input points. By carefully specifying this covariance structure, the Gaussian process can capture and model the underlying smoothness of the system, allowing for accurate predictions and insights even when faced with limited or noisy data. Usually, the selection of the covariance functional form or kernel ($k(\boldsymbol{x}, \boldsymbol{x}')$ in Equation (4)) is primarily driven by assumptions regarding the underlying function to be modeled. Similar works in the literature (Gentile and Galasso, 2020; Sarli *et al.*, 2022) have adopted the squared exponential covariance function. However, In this study, the Matern 5/2 demonstrated a better performance.

Model Performance

To assess the model's performance, the Root Mean Square Error (RMSE) is employed, serving as a measure of the error rate of the regression model. A smaller RMSE value signifies a smaller deviation between the predicted and actual values. Additionally, the evaluation of the model extends to include other metrics as described here:

- The coefficient of determination (R^2) is utilized, which ranges between 0 and 1, with higher values indicating better fitting.
- Mean Bias Error (MBE) is a metric used to measure the bias or systematic error in a model's predictions. It quantifies the average difference between the predicted values and the actual values in a dataset. In other words, it identifies whether the model tends to overpredict or underpredict and by how much on average.
- Mean Absolute Error (MAE) measures the average magnitude of the errors between predicted values and actual values in a dataset. MAE gives equal weight to all errors, regardless of whether they are positive (overpredictions) or negative (underpredictions), which makes it less sensitive to outliers.

By considering these metrics, a comprehensive evaluation of the model's accuracy and predictive capability can be achieved. Table 2 shows the error values for eight different GP processes.

Table 2. Validation and test error values for eight GPs (four fragility medians and four beta)

GP Model	Stage	Med [PGA in g]				Beta			
		RMSE	R^2	MBE	MAE	RMSE	R^2	MBE	MAE
DS1	Validation	0.0032	0.99	-0.0001	0.002	0.014	0.81	0.0003	0.01
	Test	0.0027	0.99	0.0006	0.002	0.012	0.92	-0.003	0.011
DS2	Validation	0.013	0.98	0.0003	0.008	0.01	0.94	0.0007	0.007
	Test	0.014	0.99	0.0004	0.01	0.011	0.94	0.002	0.009
DS3	Validation	0.003	0.99	-0.0002	0.002	0.006	0.98	0.0005	0.004
	Test	0.004	0.99	0.002	0.003	0.007	0.98	0.005	0.005
DS4	Validation	0.004	0.99	0.0002	0.003	0.006	0.98	0.005	0.004
	Test	0.007	0.99	0.003	0.004	0.007	0.98	-0.005	0.006

4 Conclusion

In this paper, we elaborated on the procedure and results of a ML-based surrogate model that can be implemented as a submodule in a Multi-Hazard Risk Management decision support tool. This model can assess the effects of different retrofit measures for URM buildings in terms of changes in fragility curves. We used the capacity curves of 390 buildings (un-retrofitted and retrofitted) that were developed by a robust analytical-mechanical procedure (DBV-Masonry) and performed a modified cloud analysis to drive their fragility functions. Then, eight Gaussian Processes (GP) were trained to map the capacity curve parameters to the fragility function parameters. The results are promising as they show an acceptable accuracy while requiring a very small computation power and time, which makes it a perfect solution for the evaluation of city-wide retrofit scenarios. There are, however, some areas that authors are currently trying to improve. First, the sensitivity of the results to record selection for cloud analysis and utilization of other Intensity Measures (considering that the results will be used to assess a city-wide portfolio of buildings) are being investigated. Furthermore, since the initial results of other ML methods (such as neural networks) are in an acceptable range, the possibility of combining several ML methods to cover each other's weaknesses is under investigation.

5 Acknowledgment

The authors would like to express their gratitude to Professor Sergio Lagomarsino and Dr. Andrea Brunelli for providing the cyclic pushover results that were used to calibrate the pinching4 material model.

6 References

Baraschino, R., Baltzopoulos, G. and Iervolino, I. (2020) 'R2R-EU: Software for fragility fitting and evaluation of estimation uncertainty in seismic risk analysis', *Soil Dynamics and Earthquake Engineering*, 132, p. 106093.

Bernardini, A., Gori, R. and Modena, C. (1990) 'An application of coupled analytical models and experiential knowledge for seismic vulnerability analyses of masonry buildings', *Engineering aspects of earthquake phenomena*, 3, pp. 161–180.

Blasi, G., Perrone, D. and Aiello, M.A. (2023) 'Fragility curves for reinforced concrete frames with retrofitted masonry infills', *Journal of Building Engineering*, p. 106951.

Cattari, S. *et al.* (2021) 'Comparative study on two analytical mechanical-based methods for deriving fragility curves targeted to masonry school buildings', in *Proceedings of the 8th ECCOMAS Thematic Conference on Computational Methods in Structural Dynamics and Earthquake Engineering, Athens, Greece*, pp. 28–30.

Cattari, S. *et al.* (2022) 'Risk assessment of Italian School buildings at national scale: the MARS project experience', in *Proceedings of 3rd European Conference on Earthquake Engineering and Seismology, 3ECEES, Bucharest, Romania, September 4th to 9th*.

Cornell, C.A. *et al.* (2002) 'Probabilistic basis for 2000 SAC federal emergency management agency steel moment frame guidelines', *Journal of structural engineering*, 128(4), pp. 526–533.

Delaviz, A. and Yaghmaei-Sabegh, S. (2023) 'Development of a new framework based on Gaussian regression process for rapid fragility analysis of 2-DoF base-isolated structures', in *Structures*. Elsevier, pp. 1135–1149.

Fayaz, J. *et al.* (2023) 'Assessment of ground motion amplitude scaling using interpretable Gaussian process regression: Application to steel moment frames', *Earthquake Engineering & Structural Dynamics* [Preprint].

Ferreira, T.M., Maio, R. and Vicente, R. (2017) 'Analysis of the impact of large scale seismic retrofitting strategies through the application of a vulnerability-based approach on traditional masonry buildings', *Earthquake Engineering and Engineering Vibration*, 16(2), pp. 329–348.

Follador, V. *et al.* (2023) 'Effect of retrofit interventions on seismic fragility of Italian residential masonry buildings', *International Journal of Disaster Risk Reduction*, 91, p. 103668.

Gentile, R. and Galasso, C. (2020) 'Gaussian process regression for seismic fragility assessment of building portfolios', *Structural Safety*, 87, p. 101980.

Hoyos, M.C. and Silva, V. (2022) 'Exploring benefit cost analysis to support earthquake risk mitigation in Central America', *International Journal of Disaster Risk Reduction*, 80, p. 103162.

Italian Ministry of Infrastructures and Transports (2019) *Circolare no. 7 C.S.LL.PP. of 2009/01/21 (GU n.35 del 11-2-2019 - suppl. Ordinario n. 5)*.

Jafari, S. and Mahini, S.S. (2023) 'Enhancement of the Fragility Capacity of RC Frames Using FRPs with Different Configurations at Joints', *Polymers*, 15(3), p. 618.

Jalayer, F. *et al.* (2017) 'Analytical fragility assessment using unscaled ground motion records', *Earthquake Engineering & Structural Dynamics*, 46(15), pp. 2639–2663.

Jalayer, F., De Risi, R. and Manfredi, G. (2015) 'Bayesian Cloud Analysis: efficient structural fragility assessment using linear regression', *Bulletin of Earthquake Engineering*, 13, pp. 1183–1203.

Kalakonas, P. and Silva, V. (2022) 'Seismic vulnerability modelling of building portfolios using artificial neural networks', *Earthquake Engineering & Structural Dynamics*, 51(2), pp. 310–327.

Kuehn, N.M. and Abrahamson, N.A. (2020) 'Spatial correlations of ground motion for non-ergodic seismic hazard analysis', *Earthquake Engineering & Structural Dynamics*, 49(1), pp. 4–23.

Lagomarsino, S. *et al.* (2013) 'TREMURI program: an equivalent frame model for the nonlinear seismic analysis of masonry buildings', *Engineering structures*, 56, pp. 1787–1799.

Lagomarsino, S. and Cattari, S. (2014)' Fragility functions of masonry buildings Chapter 5 of Syner-G: Typology definition and fragility functions for physical elements at seismic risk Pitilakis K, Crowley H, Kaynia A'. Springer.

Lagomarsino, S. and Giovinazzi, S. (2006) 'Macroseismic and mechanical models for the vulnerability and damage assessment of current buildings', *Bulletin of Earthquake Engineering*, 4, pp. 415–443.

Lavrentiadis, G. *et al.* (2022) 'Overview and introduction to development of non-ergodic earthquake ground-motion models', *Bulletin of Earthquake Engineering*, pp. 1–30.

Manfredi, V. *et al.* (2022) 'Selection and spectral matching of recorded ground motions for seismic fragility analyses', *Bulletin of Earthquake Engineering*, 20(10), pp. 4961–4987.

Martins, L. *et al.* (2021) 'Vulnerability Modellers Toolkit, An Open-source Platform for Vulnerability Analysis'.

MathWorks, M. (2023) 'Statistics and machine learning Toolbox™ user's guide'. The MathWorks Natick.

Miano, A. *et al.* (2018) 'Cloud to IDA: Efficient fragility assessment with limited scaling', *Earthquake Engineering & Structural Dynamics*, 47(5), pp. 1124–1147.

Minas, S., Chandler, R.E. and Rossetto, T. (2018) 'BEA: An efficient Bayesian emulation-based approach for probabilistic seismic response', *Structural Safety*, 74, pp. 32–48.

Padgett, J.E. and DesRoches, R. (2008) 'Methodology for the development of analytical fragility curves for retrofitted bridges', *Earthquake Engineering & Structural Dynamics*, 37(8), pp. 1157–1174.

Pang, Y. *et al.* (2021) 'Uniform design–based Gaussian process regression for data-driven rapid fragility assessment of bridges', *Journal of Structural Engineering*, 147(4), p. 4021008.

Pietro, C., Veronica, F. and Marco, D. (2023) 'Effectiveness of seismic mitigation strategies for the Italian masonry building heritage', *Procedia Structural Integrity*, 44, pp. 1752–1759.

da Porto, F. *et al.* (2021) 'Comparative analysis of the fragility curves for Italian residential masonry and RC buildings', *Bulletin of Earthquake Engineering*, 19(8), pp. 3209–3252.

DA PORTO, F. *et al.* (2022) 'Fragility curves of as-built and retrofitted masonry buildings in Italy', in *Proceedings of the Third European Conference on Earthquake Engineering and Seismology–3ECEES*, pp. 3337–3346.

Rasmussen, C.E. and Williams, C.K.I. (2006) *Gaussian processes for machine learning*. Springer.

Saretta, Y., Sbrogio, L. and Valluzzi, M.R. (2021) 'Seismic response of masonry buildings in historical centres struck by the 2016 Central Italy earthquake. Calibration of a vulnerability model for strengthened conditions', *Construction and Building Materials*, 299, p. 123911.

Sarli, P.W. *et al.* (2022) 'Gaussian Process Regression for Seismic Fragility Assessment: Application to Non-Engineered Residential Buildings in Indonesia', *Buildings*, 13(1), p. 59.

Schulz, E., Speekenbrink, M. and Krause, A. (2018) 'A tutorial on Gaussian process regression: Modelling, exploring, and exploiting functions', *Journal of Mathematical Psychology*, 85, pp. 1–16.

Sistani Nezhad, R., Kabir, M.Z. and Banazadeh, M. (2022) 'Strength Evaluation of Masonry Walls Externally Bonded Using FRP Fabrics Under Out-of-Plane Loading Through Fragility Curves', *International Journal of Civil Engineering*, 20(12), pp. 1397–1414.

Suarez, D. *et al.* (2023) 'Gaussian process regression-based surrogate modelling for direct loss-based seismic design of low-rise base-isolated structures', *Procedia Structural Integrity*, 44, pp. 1728–1735.

Tamhidi, A. *et al.* (2022) 'Conditioned simulation of ground-motion time series at uninstrumented sites using Gaussian process regression', *Bulletin of the Seismological Society of America*, 112(1), pp. 331–347.

Valluzzi, M.R., Follador, V. and Sbrogiò, L. (2023) 'Vulnus Web: A Web-Based Procedure for the Seismic Vulnerability Assessment of Masonry Buildings', *Sustainability*, 15(8), p. 6787.

Yurdakul, Ö. *et al.* (2023) 'Fragility functions for fiber-reinforced polymers strengthened reinforced concrete beam-column joints', *Engineering Structures*, 279, p. 115570.

Zhong, J. *et al.* (2020) 'Risk-informed sensitivity analysis and optimization of seismic mitigation strategy using Gaussian process surrogate model', *Soil Dynamics and Earthquake Engineering*, 138, p. 106284.

Zhu, M., McKenna, F. and Scott, M.H. (2018) 'OpenSeesPy: Python library for the OpenSees finite element framework', *SoftwareX*, 7, pp. 6–11.